FROM THE HEALTH PHYSICS AND MEDICAL DIVISION (DIRECTOR: N. G. STEWART), ATOMIC ENERGY RESEARCH ESTABLISHMENT, HARWELL, BERKS, ENGLAND.

SYSTEMATIC ARC CALIBRATION METHOD FOR BODY RADIOACTIVITY MEASUREMENT

by

A. L. LILLEGRAVEN and J. RUNDO

The establishment of absolute correspondence between body activity content and instrument response is a major problem in whole body counting techniques (MARINELLI et coll. 1955, MILLER & MARINELLI 1956, RUNDO 1958, 1962). The most rigorous calibration method consists in injecting a known amount of the nuclide into the subject, or into another person of similar build, and measuring the response at an appropriate point in time. However, this may at worst be inadmissible and is at best not very convenient. Other less rigorous methods must therefore often be employed.

Arc calibration methods. The so-called arc method, in which the subject is placed in such a position that the body is bent along an arc of a certain radius, is commonly employed. The detector is placed at the centre of the defining circle. Its response to radiation from different parts of the body is largely equalized, and the body activity may be simulated to a good approximation by a point source embedded in a phantom; this must have a form and consistency to simulate absorption and scattering by the 'average' or a more specific body section.

Submitted for publication 11 November 1964.

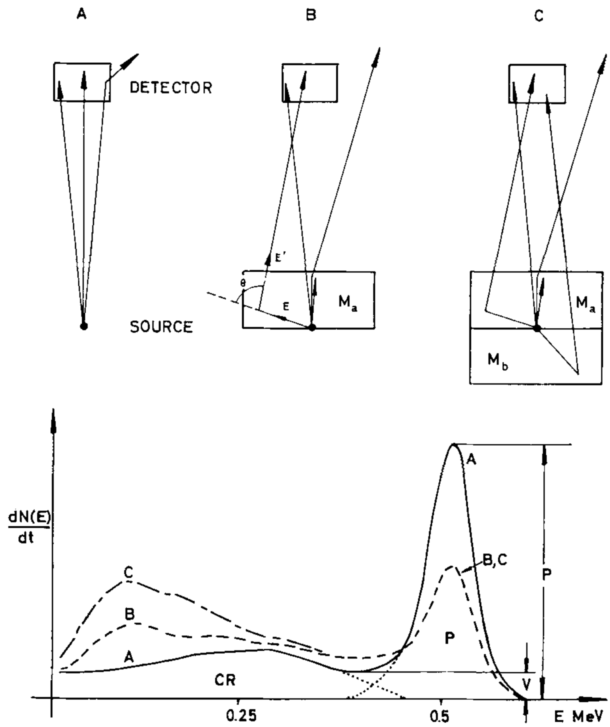

Fig. 1. Effects on the gamma-ray spectrum due to absorption and scattering in phantom material (E = 0.51 MeV in example).

The uniformity of response in depth increases with radius, and this applies also to the comfort of the person being measured. The counting efficiency, on the other hand, decreases sharply with increasing radius. A compromise must be decided upon, and in practical cases the radius may be between 1 and 2 m (Evans 1937, Marinelli et coll. 1955, Miller 1962).

Phantom considerations. The choice of a phantom involves selection of a matrix material as well as shape for the building blocks. After these decisions have been made, it remains to determine the overall dimensions and the position of the point source within the phantom.

If the measuring equipment does not permit gamma-ray energy analysis, and no knowledge of the nuclide distribution is at hand, average conditions must be assumed, i. e. the matrix thickness is set equal to the average body thickness and the point source is placed at the centre. Normally the dis-

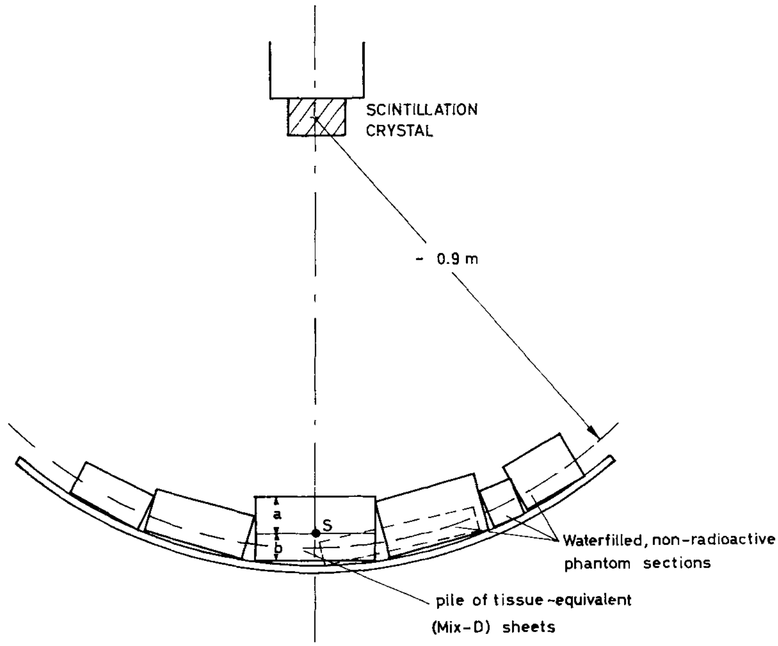

Fig. 2. Arrangement of phantom on the arc. S — source, a — number of sheets (= cm) above S, b — number of sheets below S.

tribution in the body will be known to some extent and this knowledge is taken into account.

When a gamma-ray spectrometer is available, however, spectrum modifications due to the phantom will provide additional information which may be used to determine phantom dimensions and source positioning.

Effects of the phantom on spectral shapes. The spectral modifications taking place when absorbing and scattering material is introduced in the source surroundings are illustrated in Fig. 1. Spectrum A, obtained when essentially no absorption and scattering takes place outside the scintillation crystal, is regarded as the basic spectrum. The photopeak *P* corresponds to incident photons totally absorbed in the crystal, while the Compton region *CR* is produced by single- or multiply-scattered photons leaving the crystal volume within wide energy limits.

The spectral changes introduced by adding material M_a in front of the source (see *B*, Fig. 1) are mainly due to (1) absorption (including scattering out of beam) and degradation, and (2) forward scattering into the beam.

Referred to the basic spectrum, the main changes caused by (1) and (2) are, respectively, (I) proportionate reduction of whole spectrum, and an increase at low energies (~ 0.1 MeV), and (II) a relative increase in the number of counts in the Compton region, especially at energies a little below the primary quantum energy.

For M_a thicknesses of practical interest, the net effect of (I) and (II) is an increased counting rate in the Compton region, and a decreased counting rate in the photopeak. The modified spectrum is shown in the figure (curve B).

The only effect of adding further material M_b behind the source spectrum C is, relative to spectrum B, an enhanced counting rate in the low energy region. Curve C in Fig. 1 indicates the modification due to M_b.

Criteria for stipulating best simulation. A method introduced by MILLER & MARINELLI (1956), in which the spectrum from the subject is matched with that obtained from a point source buried in a Presdwood phantom, will now be considered. Material is added in front of and behind the source until the phantom spectrum is similar to that of the subject. The radioactive content of the subject is finally determined by simple proportion. The criteria for spectrum matching are not stated quantitatively.

The ultimate criterion for full similarity would be complete matching channel by channel over the entire spectrum. Such a criterion can only be fulfilled if we assume a spectral continuum and no statistical fluctuations. Even allowing for statistics and the finite number of channels, matching would often not be feasible without having recourse to distributed sources in elaborately shaped phantoms. Simpler but carefully chosen criteria must be employed in practice.

The peak-to-valley ratio (p/v, Fig. 1) has been proposed as giving a sensitive measure of the amount of material covering the source, e. g. to differentiate between surface and internal contamination (RUNDO 1958). While this effect may be used in many cases, doubts may be raised as to the value of this quantity in cases of low body radioactivity, as it is also very susceptible to statistical fluctuations.

A systematic method with simplified criteria for matching body and phantom spectra will now be described.

Systematic calibration method

The phantom is built up as illustrated in Fig. 2. One section of the phantom is a pile of tissue-equivalent sheets (mix-D), each $29.5 \times 29.5 \times 1$ cm, with a 'point' source placed centrally in one of them. The numbers of sheets (or

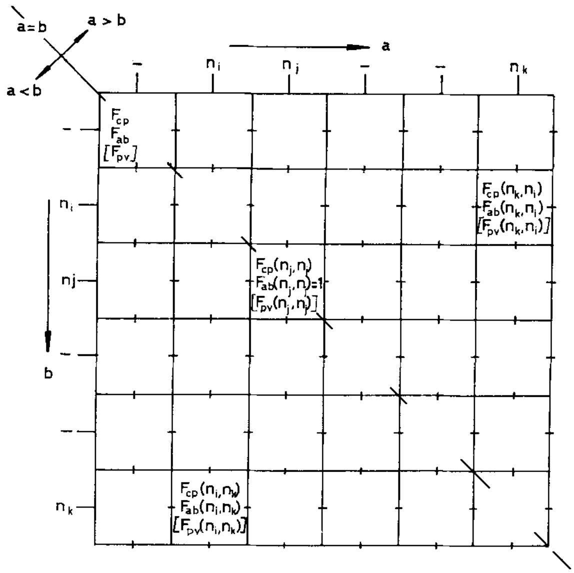

Fig. 3. Tables of spectrum indices (see text for explanation).

centimetres of material) above and below the source are denoted a and b, respectively.

Calibration spectra are recorded systematically for all combinations (a, b) within reasonable ranges of a and b, and the following quantities are extracted from each spectrum:

the total counting rate $R_p\ (a, b)$ in the photopeak;

the ratio $F_{cp}(a,b) = R_c(a,b)/R_p(a,b)$, where $R_c(a,b)$ is the total counting rate in the Compton region;

the peak-to-valley ratio $F_{pv}(a,b)$; and finally, for all combinations $(a = n_i,\ b = n_k)$ and the 'symmetrical' combinations $(a = n_k,\ b = n_i)$, values are calculated of the ratio,

$$F_{ab}(n_i, n_k) = \frac{R_p\ (n_i, n_k)}{R_p\ (n_k, n_i)}.$$

Obviously,

$$F_{ab}\ (n_k, n_i) = \frac{1}{F_{ab}\ (n_i, n_k)}, \text{ and } F_{ab}\ (n_j, n_j) = 1 \text{ by definition.}$$

These quantities are next recorded in tabular form, as indicated in Fig. 3. Now, by interpolation along horizontal (b = const) and/or vertical (a =

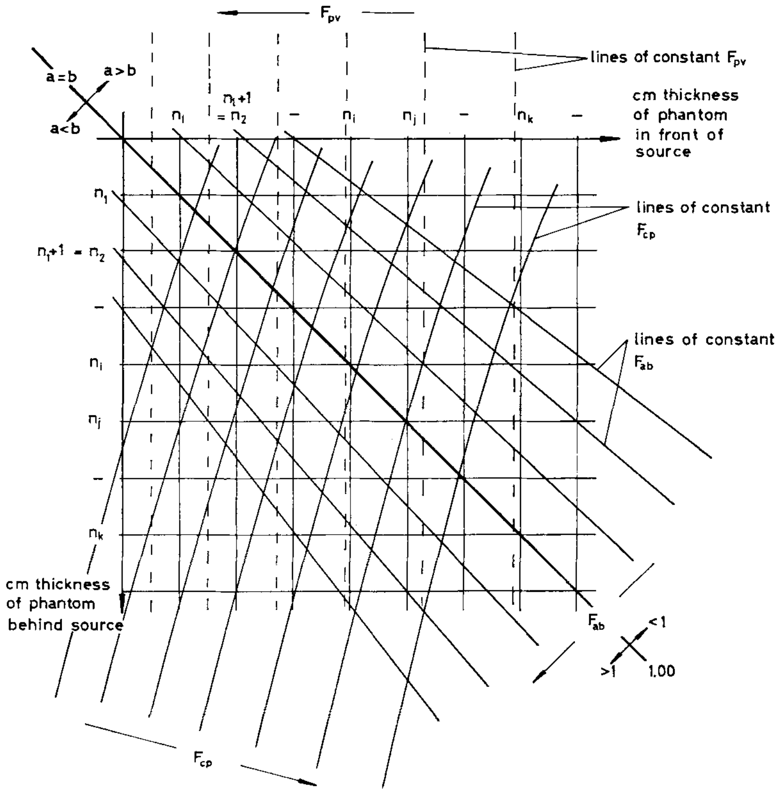

Fig. 4. Calibration chart derived from fig. 3.

const) lines, these tabulated values may be converted into a more useful calibration chart. The latter, shown in Fig 4, displays lines of constant F_{cp}, F_{ab} (and F_{pv}) .

Use of calibration chart. The subject whose body radioactivity content is to be determined, is measured twice in the arc arrangement, once on the back and once on the front. The quantities ${}^fF_{cp}$, ${}^bF_{cp}$, ${}^fF_{ab}$ $(= {}^fR_p/{}^bR_p)$ and ${}^bF_{ab} = {}^fF_{ab}^{-1}$ (if desired also ${}^fF_{pv}$ and ${}^bF_{pv}$) (where the superscripts f and b denote 'on front' and 'on back') are determined.

The point-source/phantom-simulation method implies, as do all related calibration methods, that full matching of body and phantom spectra is tantamount to equivalence between total body and point source activities. Furthermore, as linearity between detector response and the activity in any

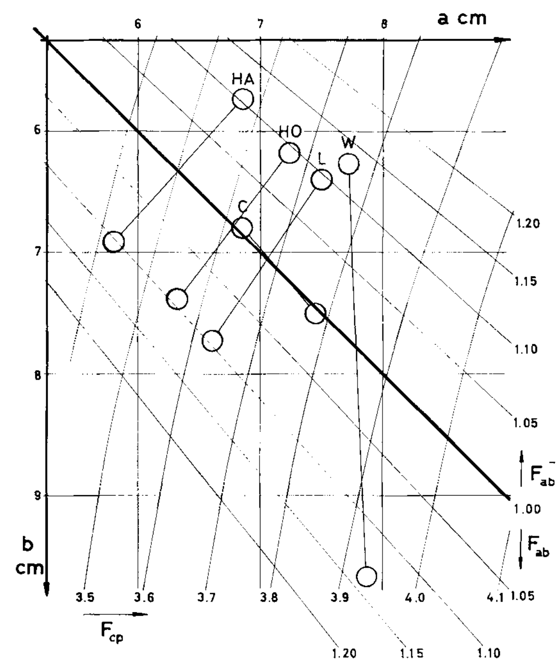

Fig. 5. Calibration points for five subjects containing strontium 85.

fixed geometry may normally be taken for granted, simple proportion applies in the general case of spectral similarity alone, i. e.

$$s = \frac{r}{R(a,b)} S \tag{1}$$

where s and S are subject and point-source activities, and r and $R(a,b)$ integral counting rates over any region common to the subject and phantom spectra, respectively. (Total counting rate or photopeak counting rate are practical choices.)

If we now plot the point $({}^fF_{ab},{}^fF_{cp})$ on the calibration chart, the corresponding phantom combination (a_1,b_1) — a and b will generally not be integers, and $R(a,b)$ is found by interpolation — may be read directly and the body content s' may be determined from eq. (1). Also point $({}^bF_{ab}, {}^bF_{cp})$ selects a combination (a_2, b_2) on the chart and a value s'' for the body content. Ideally $({}^bF_{ab}, {}^bF_{cp})$ must be positioned symmetrically to $({}^fF_{ab}, {}^fF_{cp})$ with respect to the diagonal corresponding to $a = b$. Turning of the subject corresponds to turning of the phantom, consequently $(a_2, b_2) = (b_1, a_1)$, symmetrical to (a_1, b_1). It necessarily follows from this that s'' is equal to s'.

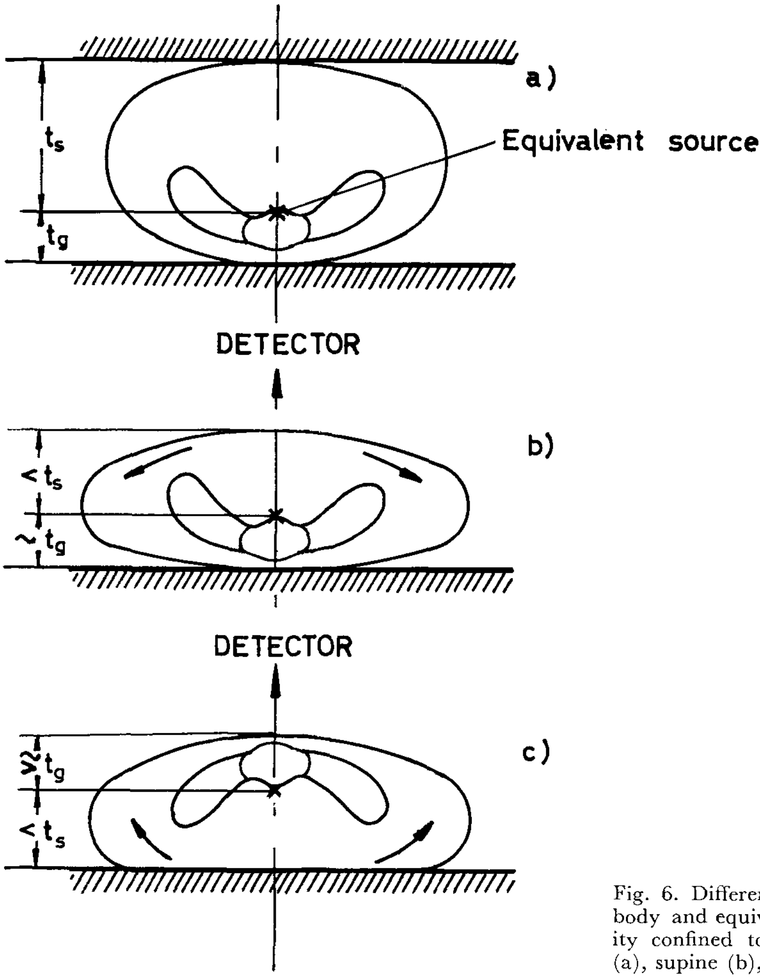

Fig. 6. Different configurations of body and equivalent source (activity confined to skeleton): standing (a), supine (b), and prone (c).

Experimental. The ^{85}Sr contents of five human subjects had to be determined in the course of strontium retention studies (RUNDO et coll. 1964) carried out in collaboration with G. E. Harrison of the Medical Research Council's Radiobiological Research Unit, Harwell, England. The measurements took place some days after the cessation of the intake period, and it could therefore be assumed that nearly all the strontium (a bone-seeking nuclide) was deposited in the skeleton.

From the net ^{85}Sr spectra, indices $^fF_{ab}$, $^bF_{ab}$ $(= {^fF_{ab}}^{-1})$, $^fF_{cp}$ and $^bF_{cp}$ were extracted and plotted on a ^{85}Sr

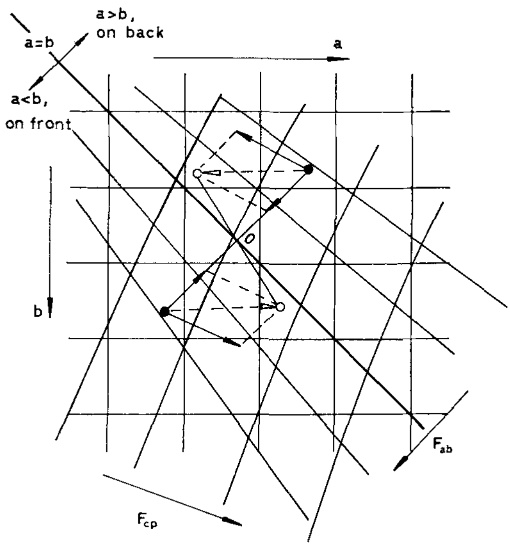

Fig. 7. Effects of body elasticity. Solid circles are symmetrical calibration points, in the ideal case of the rigid body; open circles are calibration points for the elastic body.

calibration chart, according to the method described above (Fig. 5). Conjugate points are interconnected.

Deviation from symmetry. It appears from Fig. 5 that the symmetry rule applies well for three of the point pairs, viz *HA*, *HO* and *L*, whereas cases *C* and *W* differ markedly. No attempts will be made to discuss in full the reasons for the discrepancy. These have to do with the range of validity of the simulation method itself, the assessment of which is difficult. However, attention is drawn to an effect which is easily deduced qualitatively and which may account very largely for the observed differences.

The calibration method requires turning of the body from the prone to the supine position. Obviously, it also demands that all body sections are rigid during this process, i. e. no sagging within the body is allowed, by analogy with the phantom. In practice the elasticity of the human body must be accepted as a fact and an attempt will be made to evaluate its effect on the calibration.

The activity is deposited in the skeleton in the particular examples discussed and it will be assumed that the spine and the hip-bones are the parts of the skeleton most affected by lack of rigidity. 'Average' body cross-sections are outlined in Fig. 6, in an exaggerated manner, for three different postures: the erect body is illustrated in (a), and in the others the body lying on the arc stretcher in supine (b) and prone (c) positions, respectively. It may be assumed in relation to the spectrum for the rigid body that the spectra from the non-rigid body should deviate as illustrated below:

Body position	Effect on the body	Effect on the gamma spectrum	Effect on the calibration indices
Supine	Source-detector distance little affected; less absorbing material between activity and detector	Photopeak larger; probably the same or lower Compton region	Decrease of $F_{cp}=\frac{R_c}{R_p}$
Prone	Source-detector distance larger; forward scattering volume increased; back-scattering volume decreased	Photopeak smaller: Compton region probably the same or higher	Increase of $F_{cp}=\frac{R_c}{R_p}$
Combined, assuming ${}^fF_{ab} > {}^bF_{ab}$ for a bone-seeking nuclide:			${}^fF_{ab}$ will decrease and ${}^bF_{ab}$ increase

The resulting deviations are depicted graphically in Fig. 7.

If we now compare the derived deviation with that observed for cases *C* and *W*, it is evident that both go in the same direction. Cases *HA*, *HO* and *L* also display the same tendency, but little reliance can be placed on this as the deviations are of the same order of magnitude as the statistical fluctuations. — It should be noted that in all cases ${}^fR_p > {}^bR_p$, or ${}^fF_{ab} > 1$, i. e. more of the body activity is positioned near the back. This is contrary to observations made by MILLER & MARINELLI (1956) on the distribution of ^{226}Ra, another bone-seeker, but in agreement with their findings with ^{85}Sr.

Pursuing this line of reasoning, one will expect the magnitude of the deviation to be a function of body elasticity. More specifically, less rigidity will lead to larger deviations. Such a tendency may be deduced from Fig. 5, if we accept a relationship between body softness and body thickness.

One way of obtaining a relative measure for the average body thickness is to calculate the ratio W/H, where W and H are body weight and height, respectively.

Another measure of body thickness is inherent in the diagram of Fig. 5. A phantom combination (a, b) with a total thickness $a + b$ corresponds to each calibration point. Average thickness deduced from two conjugate points, $((a + b)_f + (a + b)_b)/2$, is very nearly equal to that derived from the intersection point between the interconnecting line and the diagonal $a = b$; the latter is chosen for the sake of convenience. The existence of a positive correlation between W/H and $(a + b)$ is apparent from Fig. 8, and it is noteworthy that the straight line drawn between the points passes through the origin. This indicates that W/H may be a sensible measure of body thickness

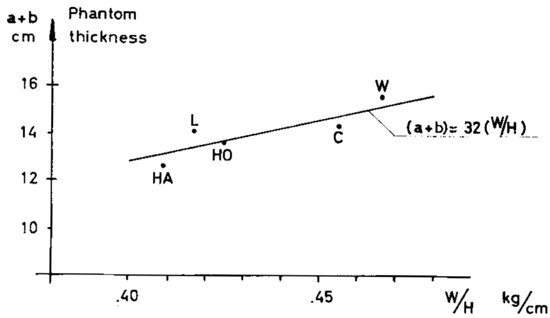

Fig. 8. Correlation between two different measures of body thickness.

in this case, although, because both the distance of the points from the origin and the scatter about the line are considerable, it is not definite. ($\sqrt{W/H}$ would be a more correct measure presuming exact axial proportionality between bodies of all sizes. However, proportionality is certainly not a firm rule, and with large values of W/H the trunk is liable to be mainly responsible.)

Returning to the considerable deviation from symmetry in cases C and W, it is evident from Fig. 8 that they also form a separate group with respect to body thickness as measured by W/H. This strongly suggests that body elasticity is the principal phenomenon responsible for non-symmetry.

Determination of the body activity. This is described under subheading 'Use of calibration chart' for cases where the two calibration points are symmetrical to each other. In all other cases s' and s'' will differ and the body content is then set equal to $s_{av} = \frac{s' + s''}{2}$. If F_{ab} is not too different from unity, however, another and more convenient procedure may be used.

Both calibration points are displaced by an equal amount in Fig. 7, as this seems reasonable when no quantitative knowledge on the displacement mechanism is at hand. However, one point remains fixed during the displacement, viz. the point of intersection 0 between the diagonal ($a = b$) and the interconnecting line. It can be shown, with reasonable assumptions, that the body content is given approximately by the expression

$$s = \frac{\frac{1}{2}\,({}^{f}r_p + {}^{b}r_p)}{R_p\,(n_j,\, n_j)}\, S \tag{2}$$

where ${}^{f}r_p$ and ${}^{b}r_p$ are body photopeak counting rates on the front and on the back respectively, $R_p(n_j, n_j)$ is the phantom photopeak counting rate corresponding to the pivot point 0, and S is the activity of the point source.

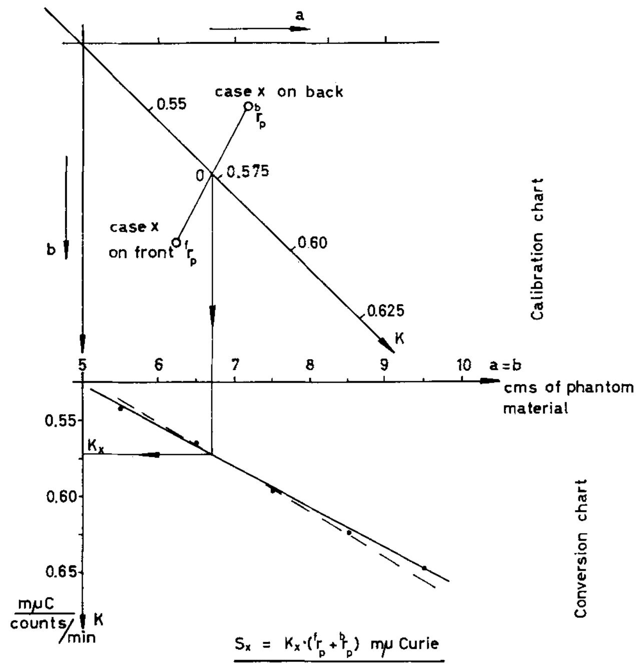

Fig. 9. Simplified determination of radioactive content of body. The measurement points (·) determine the calibration line (continuous). The broken line shows the theoretical slope.

Eq. (2) invites an extension of the calibration chart, making the activity determination very simple. If eq. (2) is arranged as follows:

$$s = ({}^{f}r_p + {}^{b}r_p)\cdot\frac{S}{2\,R_p\,(n_j,\,n_j)} = ({}^{f}r_p + {}^{b}r_p)\cdot K,$$

it becomes evident that the diagonal may be calibrated directly in terms of $K\,\dfrac{n\text{Ci}}{\text{counts/min}}$. A conversion chart may also be put beneath the calibration chart. Both alternatives are shown in Fig. 9. The conversion line illustrated in this diagram is that obtained from the actual ^{85}Sr calibration measurements.

A theoretical calibration line has also been drawn; this is derived from

$$K = C\,(90 - n_j)^2\,\exp(\sigma n_j),$$

where n_j is the half-thickness of the phantom and σ is the linear absorption coefficient of the phantom material; C is a factor which is a function of the size of the crystal, and of the gamma ray energy. The line drawn in Fig. 9 was forced through the centre of gravity of the measured points by adjusting the value of C. The difference between the theoretical and measured slopes may be largely due to an increased contribution to the measured photopeak counting rates from forward scattered gamma rays, as the relative contribution increases with increasing phantom thickness (see Fig. 1, curves A and B).

Discussion

Calibration of whole body counting arrangements by phantom/body spectral matching appears to be a well established method. Normally the body spectrum is measured first, followed by a trial-and-error procedure, in which the phantom is rearranged until its spectrum matches that of the body. The criteria for matching may differ, and are not always firmly defined.
The procedure described in this paper differs in two respects:

A. Phantom spectra are first recorded systematically and are used for preparing a calibration chart. This chart is used for all subsequent body activity measurements on the same nuclide, provided no drastically different geometry or distribution is encountered;

B. The use of the quantities F_{cp} and F_{ab} as spectrum indices for assessing spectral matching.

Doubts may be raised as to the practicality of preparing a calibration chart if only a few cases are to be measured. We have however found that the time required is not too long when a reasonably strong source is employed, and the use of a modern multi-channel pulse amplitude analyser with 'sophisticated' read-out equipment facilitates the accumulation of the necessary data.

No claim is made for the ultimate advantages of F_{cp} and F_{ab} as spectrum descriptors. They reflect features of the spectrum that seem to be reasonably susceptible to differences in distribution of the activity and in body shapes. At the same time they can be determined with fairly high precision even when the statistical fluctuations on individual channel counting rates are considerable. The lines of constant F_{cp} cross those of constant F_{ab} at angles approaching 90°, as may be seen from Fig. 5, and this is of considerable help as regards resolution of the calibration points. Nevertheless better indices may certainly be found by consideration of the discussion on the effects of the phantom on spectral shapes.

Inevitably, there must be a limit as to how much information may be extracted. Improvements will change from real to superficial ones when the possibilities of the single point source phantom are exhausted. The arc method is however valuable because of its simplicity, and further investigations into its range of validity should be welcomed.

Addendum in proofs

Since this paper was submitted for publication we have obtained some evidence of the accuracy of the method. An intravenous injection of 2.25 μCi of barium 133 was administered to a volunteer subject; body radioactivity measurements were made using a crystal 9 inches in diameter by 6 inches thick and an arc radius of 170 cm, and a calibration chart was prepared as described in the text. The results obtained are compared with those from measurements of the cumulative excretion in the following table. During the 13 days follow-

Days after injection	(A) Body content μCi	(B) Cumulative excretion μCi	$\frac{A}{2.25-B}$
0	2.10	0	0.93_5
1	1.49	0.65	0.93
2	0.86	1.29	0.90
3	0.58	1.64	0.95
4	0.47	1.71	0.87
6	0.34	1.88	0.92
8	0.29	1.94	0.93_5
10	0.25	1.98	0.92_5
13	0.22_6	2.01	0.94

ing injection the value of K varied unsystematically between 0.42 and 0.47 $\frac{n\text{Ci}}{\text{counts/min}}$; there appears to be a systematic error in estimating the body content but this only exceeded 8 per cent on two occasions. When the results are converted to percentage retention i.e. 100A/2.10 and 100-100B/2.25, the agreement is excellent.

Acknowledgements

This work was carried out while one of us (A.L.L.) was on leave of absence from the Norwegian Defence Research Establishment, Kjeller, Norway, financed by N.D.R.E. and by a research fellowship from the Royal Norwegian Council for Scientific and Industrial Research. We wish to thank Miss J. I. Mason for the help with measurements of gamma ray spectra from the phantom. Mr P. D. Cross made the measurements of gamma ray spectra from the phantom and prepared the calibration chart mentioned in the addendum.

SUMMARY

In the arc technique for calibrating whole body counting arrangements, the radiation emitted by the body is simulated by that from a point source in a phantom. A procedure is described in which phantom spectrum information is extracted systematically and then used for preparing a calibration chart which can be employed in all subsequent body activity measurements of the same nuclide. Its application is illustrated by the results of measurements on five human subjects after their intake of strontium 85.

ZUSAMMENFASSUNG

Es wird eine Methode beschrieben, die es erlaubt systematisch Phantomspectrumdaten zu erhalten, und mit der es dann möglich ist eine Kalibrierungstabelle für spätere Aktivitätsmessungen desselben Nuklides aufzustellen. Die Anwendungsmöglichkeit der Methode wird demonstriert, mit Resultaten von Messungen an 5 Personen die Strontium 85 in ihren Geweben enthielten.

RÉSUMÉ

Dans la technique de l'arc pour l'étalonnage de dispositifs de comptage de tout le corps, le rayonnement émis par le corps est simulé par celui d'une source ponctuelle située dans un fantôme. L'auteur décrit comment l'information concernant le spectre du fantôme est extraite systématiquement et utilisée pour préparer une fiche d'étalonnage qui peut servir pour toutes les mesures ultérieures d'activité corporelle du même nuclide. Son application est illustrée par les résultats de mesures sur cinq sujets humains après administration de strontium 85.

REFERENCES

EVANS R. D.: Radium poisoning. II. The quantitative determination of the radium content and radium elimination rate of living persons. Amer. J. Roentgenol. 37 (1937), 368.

MARINELLI L. D., MILLER C. E., GUSTAFSON P. F. and ROWLAND R. E.: The quantitative determination of gamma-ray emitting elements in living persons. Amer. J. Roentgenol. 73 (1955), 661.

MILLER C. E.: An experimental evaluation of multiple-crystal arrays and single crystal techniques. Proc. Symposium on Whole-Body Counting, p. 81. IAEA, Vienna 1962.

— and MARINELLI L. D.: Argonne National Laboratory Report ANL-5679 (1956), p. 21.

RUNDO J.: Body radioactivity measurement as an aid in assessing contamination by radionuclides. Proc. 2nd U.N. Int. Conf. P.U.A.E. 23 (1958), 101.

— Some calibration problems of whole-body gamma-ray spectrometers. Proc. Symposium on Whole-Body Counting, p. 121. IAEA, Vienna 1962.

— LILLEGRAVEN A. L. and MASON J. I.: The retention of strontium in man. Bone and Tooth, p. 158. Proc. First European Symposium. Pergamon, Oxford 1964.